

Laser-Induced Fluorescence Imaging

Stephen W. Allison and William P. Partridge

Introduction

Fluorescence imaging is a tool of increasing importance in aerodynamics, fluid flow visualization, and nondestructive evaluation in a variety of industrial circumstances. It is a means for producing two-dimensional images of real surfaces or fluid case-sectional areas that correspond to data on properties such as temperature or pressure across the surfaces. This article discusses three major fluorescence imaging techniques.

* Planar Laser Induced Fluorescence

* Phosphor Thermography

* Pressure Sensitive Paint

Since the 1980's, planar laser induced fluorescence (PLIF) has been used for combustion diagnostics and to characterize gas and liquid phase fluid flow situations. Depending on the application, the technique can determine species concentration, partial pressure, temperature, flow velocity, or flow distribution/visualization. Phosphor thermography is used to image surface temperature distributions. Fluorescence imaging of aerodynamic surfaces coated with phosphor material for thermometry purposes dates back to the 1940's and continues today. Imaging of fluorescence from pressure sensitive paint (PSP) is a third diagnostic approach to aerodynamic and propulsion research discussed here and it has received much attention during the past decade. These three methodologies appear to be the primary laser-induced fluorescence imaging applications outside medicine and biology. As a starting point for this article we will first discuss PLIF as it is more developed than surface LIF imaging applications.

Planar Laser Induced Fluorescence

Planar laser-induced fluorescence (PLIF) in a fluid medium is a nonintrusive optical diagnostic tool for making temporally and spatially resolved measurements. For illumination, a laser beam is formed into a thin sheet and directed through a test medium. The probed volume may contain a mixture of various gaseous constituents and the laser may be tuned to excite fluorescence from a specific component. Alternatively, the medium may be a homogenous fluid into which a fluorescing tracer has been injected. An imaging system normal to the plane of the imaging sheet views the laser-irradiated volume. Knowledge of the laser spectral characteristics, the spectroscopy of the excited material, and other aspects of the fluorescence collection optics is required for quantifying the parameter of interest.

A typical PLIF setup is shown schematically in Figure 1. In this example, taken from reference 1, an ultraviolet laser probes a flame. A long focal length spherical lens and a cylindrical lens together expand the beam and form it into a thin sheet. The spherical lens is specified to achieve the desired sheet thickness and depth of focus, the Rayleigh range, to be discussed below. An alternate method for planar laser imaging is to use the small diameter, circular beam typically emitted by the laser and scan it. Alternate sheet formation methods include combining the spherical lens with a scanned-mirror system and other scanning approaches. Fluorescence excited by the laser is collected by a lens or lens system, sometimes with intervening imaging fiber optics, and focused onto a camera's sensitive surface. In the example this is performed by a gated intensified charge coupled device (ICCD).

Background

Since its conception in the early 1980's, PLIF has grown to become a powerful and widely used diagnostic technique. The PLIF diagnostic technique evolved naturally out of early imaging research based on Raman-scattering (2), Mie-scattering, and Rayleigh-scattering along with 1-D LIF research (3). Planar imaging was originally proposed by Hartley (2), who made planar Raman-scattering measurements and termed the process Ramanography. Two-dimensional LIF based measurements were made by Miles et al. (4) in 1978. Some of the first applications of PLIF, dating to the early 1980's, involved imaging of OH in a flame. In addition to its use for

species imaging, PLIF has also been employed for temperature and velocity imaging. General reviews of PLIF have been provided by Alden and Svanberg (3), and Hanson et al. (5). Reference 6 also provides recent information on this method as applied to engine combustion. Overall, it is difficult to state in a general manner the range of the various parameters, e.g., temperature, concentration, etc. It may be noted that single molecules can be detected and temperature measured from cryogenic to combustion ranges depending on specific applications.

General PLIF Theory

The relationship between the measured parameter (e.g. concentration, temperature, pressure) and the fluorescence signal is unique to each measured parameter. However, the most fundamental relationship between the various parameters is provided by the equation describing LIF or PLIF concentration measurements. Hence, this relationship is described in a general manner below to clarify the different PLIF measurement techniques that derive from it. The equation for the fluorescence signal in volts (or digital counts on a per-pixel basis for PLIF measurements) is formulated as:

$$S_D = (V_C f_B N_T) \cdot (\Gamma_{12,L} B_{12} I_v^o) \cdot \Phi \cdot \left(\eta \frac{\Omega}{4\pi} \right) \cdot GR \Delta t_L$$

where

$$\Phi = \frac{A_{N,F}}{A_N + Q_e + W_{12} + W_{21} + Q_P}$$

and

S _D : Measured fluorescence signal	V _C : Collection volume, ie portion of laser irradiated volume viewed by detection system	f _B : Boltzmann fraction in level 1.
---	--	---

N_T : Total number density of probe species	$\Gamma_{12,L}$: Overlap fraction (i.e. energy level line width divided by laser line width.)	B_{12} : Einstein coefficient for absorption from level 1 to level 2
I_V° : Normalized laser spectral irradiance	Φ : Fluorescence yield	η : Collection optics efficiency factor
Ω : Solid angle subtended by the collection optics	G : gain of camera (applicable if it is an intensified CCD)	R : CCD responsivity
Δt_L : Temporal full width half maximum of the laser pulse	$A_{N,F}$: Spectrally filtered net spontaneous emission rate coefficient	A_N : Net spontaneous emission rate coefficient
Q_e : Fluorescence quenching rate coefficient	Q_p : Predissociation rate coefficient	W_{12} : Absorption rate coefficient
W_{21} : Stimulated emission rate coefficient		

The individual terms in Equation 1 have been grouped in a manner that provides a clear physical interpretation of the actions represented by the individual groups. Moreover, the groups have been arranged from left to right in the natural order that the fluorescence measurement progresses. The first parenthetical term in Equation 1 is the number of probe molecules in the lower laser-coupled level. This is the fraction of the total number of probe molecules, which are available for excitation. The second parenthetical term in Equation 1 is the probability per unit time that one of the available molecules will absorb a laser photon and become electronically excited. Hence, following this second parenthetical term, a fraction of the total number of probed molecules has become electronically excited and has the potential to fluoresce. More detailed explanation is contained in Reference 1.

The fluorescence yield, Φ , represents the probability that one of the electronically excited probe molecules will relax to the ground electronic state by spontaneously emitting a fluorescence photon within the spectral bandwidth of the

detection system. This fraction reflects the fact that spectral filtering is applied to the total fluorescence signal and that radiative as well as nonradiative (e.g. spontaneous emission and quenching, respectively) decay paths are available to the excited molecule. In the linear fluorescence regime and in the absence of other effects such as predissociation, the fluorescence yield essentially reduces to $\frac{A_{N,F}}{(A_N + Q_E)}$ so that the fluorescence signal is adversely affected by the quenching rate coefficient.

The third parenthetical term in Equation 1 represents the net efficiency of the collection optics. This term accounts for both reflection losses as well as the fact that only a fraction of the isotropically emitted fluorescence is captured (due to the finite solid angle of the collection optics). The next term, $\eta \frac{\Omega}{4\pi}$, is the fraction of the fluorescence emitted by the electronically excited probe molecules that impinges on the detector surface (in this case, an ICCD). This captured fluorescence is then passed through an optical amplifier where it receives a gain, G. The amplified signal is then detected with a given spectral responsivity, R. The detection process in Equation 1 produces a time varying voltage or charge (depending on whether a PMT or ICCD detector is used.) This time varying signal is then integrated over a specific gate time to produce the final measured fluorescence signal. Using Equation 1, the total number density of the probed species, N_T , can be determined via a PLIF measurement of S_D provided the remaining unknown parameters could be either calculated or calibrated.

Investigation of the different terms of Equation 1 suggests possible schemes for PLIF measurements of temperature, velocity, and pressure. For a given experimental setup (i.e. constant optical and timing parameters) and total number density of probe molecules, all of the terms in Equation 1 are constants except for f_B , $\Gamma_{12,L}$ and Q_e . The Boltzmann fraction, f_B , varies in a known manner with temperature. The degree and type of variation with temperature is unique to the lower laser-coupled level chosen for excitation. The overlap fraction, $\Gamma_{12,L}$, varies with changes in the spectral lineshape(s) of the absorption transition and/or the laser. Changes in velocity and pressure produce varying degrees of Doppler and pressure shift, respectively, in the absorption spectral profile (7-9). Hence, variations in these parameters will, in turn, produce changes in the overlap fraction. The electronic quenching rate coefficient varies with temperature, pressure, and major-species concentrations. Detailed knowledge of the relation between the

variable of interest (i.e., temperature, pressure, or velocity) and the Boltzmann fraction, f_B , and/or the overlap fraction, $\Gamma_{12,L}$, can be used in conjunction with Equation 1 to relate the PLIF signal to the variable of choice. Often ratiometric techniques can be used to allow cancellation of terms in Equation 1 that are constant for a given set of experiments. Specific examples of different PLIF measurement schemes are given in the following review of the pertinent literature.

PLIF Temperature Measurements

The theory behind PLIF thermometric measurements is the same as that developed for point LIF. Laurendeau (10) gives a review of thermometric measurements from a theoretical and historical perspective. Thermometric PLIF measurement schemes may be generally classified as monochromatic or bichromatic (two-line). Monochromatic methods employ a single laser. Bichromatic methods require two lasers in order to simultaneously excite two distinct molecular rovibronic transitions. In temporally stable environments (e.g. laminar flows), it is possible to employ bichromatic methods with a single laser by systematically tuning the laser to the individual transitions.

In bichromatic PLIF thermometric measurements, the ratio of the fluorescence resulting from two distinct excitation schemes is formed pixel-by-pixel. If the two excitation schemes are chosen such that the upper laser-coupled level (i.e., excited state) is the same, then the fluorescence yields (Stern-Vollmer factors) are identical. This is explained by Eckbreth in reference 11, an essential reference book for LIF and other laser-based flow and combustion diagnostics information. Hence, as evident from Equation 1, the signal ratio becomes a sole function of temperature through the ratio of the temperature-dependent Boltzmann fractions for the two lower laser-coupled levels of interest.

Monochromatic PLIF thermometry is based on either the thermally-assisted fluorescence (THAF) or the absolute fluorescence (ABF) methods. In THAF-based techniques, the temperature is related to the ratio of the fluorescence signals from the laser-excited level and from another higher level collisionally coupled to the laser-excited level. Implementation of this method requires detailed knowledge of the collisional dynamics, which occur in the excited level (9). In ABF-based techniques, the field of interest is uniformly doped and the fluorescence is monitored from

asingle rovibronic transition. The temperature-independent terms in Equation 1 (i.e. all terms except f_B , $\Gamma_{12,L}$ and Φ) are determined through calibration. The temperature field may then be determined from the fluorescence field by assuming a known dependence of the Boltzmann fraction, the overlap fraction and the quenching rate coefficient on temperature.

PLIF Velocity and Pressure Measurements

PLIF velocity and pressure measurements are based on changes in the absorption line-shape function of a probed molecule under the influence of variations in velocity, temperature, and pressure. In general, the absorption line-shaped function is Doppler-shifted by velocity, Doppler-broadened (Gaussian) by temperature, and collisionally broadened (Lorentzian) and shifted by pressure (10). These influences on the absorption line-shape function and consequently on the fluorescence signal via the overlap fraction of Equation 1 provide a diagnostic path for velocity and pressure measurements.

The possibility of using a fluorescence-based Doppler shift measurement to determine gas velocity was first proposed by Measures (12). The measurement strategy involved seeding a flow with a molecule, which could be excited by a visible, narrow-bandwidth laser. The Doppler-shift could be determined by tuning the laser over the shifted absorption line and comparing the spectrally resolved fluorescence to static cell measurements. By probing the flow in two different directions, the velocity vector along each propagation direction could be determined from the resulting spectrally resolved fluorescence. Miles et al. (4) used photographs to spatially resolve the fluorescence from a sodium-seeded, hypersonic nonreacting helium flow so as to make velocity and pressure measurements. The photographs of the fluorescence at each tuning position of a narrow bandwidth laser highlighted those regions of the flow with a specific velocity component. Although this work used a large diameter beam rather than a sheet for excitation, it evidently represents the first two-dimensional, LIF-based imaging measurement.

Another important method that is commonly used for visualization of flow characteristics involves seeding a flow with iodine vapor. The spectral characteristics are well characterized for iodine, enabling pressure and velocity measurement (13).

PLIF Species Concentration Measurements

The theory for PLIF concentration measurements is similar to that developed for linear LIF with broadband detection. The basic measurement technique involves exciting specific rovibronic transition of a probe molecule (seeded or naturally occurring) and determining the probed molecule concentration from the resulting broadband fluorescence. Unlike ratiometric techniques, the fluorescence signal from this single line method retains its dependence on the fluorescence yield (and therefore the electronic quenching rate coefficient). Hence, the local fluorescence signal depends on the local probe molecule number density, Boltzmann fraction, overlap fraction and electronic quenching rate coefficient. Furthermore, the Boltzmann fraction depends on the local temperature, the overlap fraction depends on the local temperature and pressure, and the electronic quenching rate coefficient depends on the local temperature, pressure and composition. This enhanced dependence of the fluorescence signal complicates determination of probed species concentrations from PLIF images. The difficulty in accurately determining the local electronic quenching rate coefficient, particularly in reacting environments, is the primary limitation to realizing quantitative PLIF concentration imaging (5). Nevertheless, methodologies for PLIF concentration measurements in quenching environments have been demonstrated based on modeling (1) and secondary measurements (2).

Useful fundamental information can be obtained from uncorrected, uncalibrated PLIF concentration images. Because of the species specificity of LIF, unprocessed PLIF images can be used to identify reaction zones, mixing regimes and large-scale structures of flows. For instance, qualitative imaging of pollutants formation in a combustor can be used to determine optimum operating parameters.

The primary utility of PLIF concentration imaging remains its ability to image relative species distributions in a plane, rather than providing quantitative field concentrations. Because PLIF images are immediately quantitative in space and time (due to the high temporal and spatial resolution of pulsed lasers and ICCD cameras, respectively), qualitative species images may be used to effectively identify zones of species localization, shock wave positions, and flame front locations (5).

The major experimental considerations limiting or pertinent to the realization of quantitative PLIF are:

1. Spatial cut-off frequency of the imaging system, which defines the range-of-scales, which can be faithfully resolved by the PLIF image;
2. Selection of imaging optics parameters (e.g., F-number and magnification) which best balance spatial resolution and signal level considerations;
3. Image corrections implemented via post processing to account for nonuniformities in experimental parameters such as pixel responsivity and offset, and laser sheet intensity; and
4. Spatial variation in the fluorescence yield due to that in the electronic quenching rate coefficient.

Laser Beam Control

A distinctive feature of planar LIF is that the imaging resolution is controlled not only by the camera and its associated collection optics but also by the laser beam optics. For instance, the thinner a laser beam is focused, the higher the resolution. This section is a simple primer for lens selection and control of beam size.

The most important considerations regarding choice of lenses are as follows. A simple lens will process light, to a good approximation, according to the thin lens equation.

$$\frac{1}{s_o} + \frac{1}{s_i} = \frac{1}{f}$$

s_o is the distance from an object to be imaged to the lens, s_i , is the distance from the lens to where an image is formed and f is the focal length of the lens as shown in Figure 2 below.

In practice, this relation is useful for imaging laser light from one plane (such as the position of an aperture or template) to another desired position in space with magnification, $M = -\frac{s_i}{s_o}$. If two lenses are used, the image of

the first lens becomes the object distance for the second. For the case of a well-collimated beam, the object distance is considered to be infinity and thus the image distance is simply the focal length of the lens. There is a limit as to how small the beam may be focused and this is termed the diffraction limit. It is given in units of length as

$w = \frac{1.22 * f * \lambda}{D}$, where λ is the wavelength of the light and D is the collimated beam diameter. If the laser

beam is characterized by a divergence, α , then the minimum spot size will be $w = f * \alpha$.

To planarize a beam, a combination of two lenses, one spherical and the other cylindrical are used. The spherical lens controls the spread and the cylindrical lens controls how thin the sheet. The result is illustrated in figure 3.

Laser-sheet formation may be accomplished via the combination of spherical and cylindrical lenses; the cylindrical lens(es) is(are) used to achieve the desired sheet height, and a spherical lens is used to achieve the desired sheet thickness and Rayleigh range. Rayleigh range is a term describing Gaussian beams (e.g., see Demtroder 7), and is the propagation distance required on either side of the beam waist to achieve a radius of $\sqrt{2}$ times the waist radius.

The Rayleigh range, z_o , is defined as $\pi \cdot w_o^2 / \lambda$, where w_o is the waist radius, and is used as a standard measurement of the waist-region length (i.e., length of the region of minimum and uniform sheet thickness). In general, longer focal length lenses produce longer Rayleigh ranges. In practice, lens selection is determined by the need to make the Rayleigh range greater than the lateral imaged distance. Since in general, longer focal length lenses produce wider sheet waist thicknesses, the specified sheet thickness and lateral image extent must be balanced.

B. Phosphor Thermography

As conceived originally, phosphor thermography was intended foremost to be a means of depicting two-dimensional temperature patterns on surfaces. In fact, over its first three decades of existence, the predominant use of the technique was for imaging applications in aerodynamics. The method was termed, "contact thermometry" since the

phosphor was in contact with the surface to be monitored. The overall approach, however, has largely been overshadowed by the introduction of modern infrared thermal imaging techniques, several of which have evolved into commercial products that are used in a wide range of industrial and scientific applications.

Fluorescence-based thermometry exploits the temperature-dependence of a fluorescence material. Usually it is an inorganic phosphor but more recently it may also be any of several organic luminescing materials. Typically, a phosphor is coated onto a surface whose temperature is to be measured. The coating is illuminated with an ultraviolet source, which induces the fluorescence. The emitted fluorescence may be captured with either a non-imaging or imaging detector. Several fluorescence properties are temperature-dependent. The fluorescence may change in magnitude and/or spectral distribution with change in temperature. Figure 4 shows a spectrum of $\text{Gd}_2\text{O}_2\text{S:Tb}$, a representative phosphor. The emission from this material originates from the rare-earth activator, Tb. The emission lines correspond to atomic transitions of Tb. At ambient temperatures, the ratio emission intensities of 410 and 490 between the mm lines changes drastically with temperature whereas other emission lines do not change until much higher temperatures are achieved. Thus the ratio indicates temperature in this range and is shown in Figure 5. Alternative phosphors are available to cover higher or lower temperatures as the case may be. Figure 6 shows a typical setup that depicts illumination either with laser light emerging from a fiber or an ultraviolet lamp. If the illumination source is pulsed, the fluorescence will persist for a period of time after the illumination is turned off. The intensity, I , will decrease, ideally according to $I = e^{-t/\tau}$ where the time required for decreasing by $1/e$ is termed the characteristic decay time, τ , sometimes also known as lifetime. The decay time is very temperature dependent and in most non-imaging applications, the decay time is measured in order to ascertain temperature. Usually for imaging, it is easier to implement the ratio method. Figure 7 shows false color images of a heated turbine blade (13). A more comprehensive description of fluorescence-based thermometry is reviewed in references 14 and 15. Temperature can be measured from about 12K to almost 2000K. In some cases, a temperature resolution of 0.01K has been achieved.

Why use phosphor thermometry when for many imaging applications infrared techniques work so well? As noted by Bizzak and Chyu, conventional thermometry methods are not satisfactory for temperature and heat transfer measurements that must be made in the rapidly fluctuating conditions peculiar to the microscale environment (16).

They suggested that thermal equilibrium on the atomic level might be achieved within 30 ns and, therefore, to be useful in performing microscale thermometry the instrumentation system must have a very rapid response time. Moreover, its spatial resolution should approach the size of an individual phosphor particle. This can be specified and may range from $< 1 \mu\text{m}$ to about $25 \mu\text{m}$. In their effort to develop a phosphor imaging system based on $\text{La}_2\text{O}_2\text{S:Eu}$, they used a frequency-tripled Nd:YAG laser. The image was split and the individual beams were directed along equal-length paths to an intensified CCD detector. The laser pulse duration was $40 \mu\text{s}$ and the ratio of the ${}^5\text{D}_2$ to ${}^5\text{D}_0$ line intensities yielded the temperature. Significantly, they were able to determine how the measurement accuracy varied with measurement area. The maximum error found for a surface the size of which was represented by a 1×1 pixel in their video system was 1.37°C , with an average error of only 0.09°C .

A particularly clever conception by Goss (17) illustrates another situation where the method is better suited than infrared emission methods. It involved the visualization of the condensed-phase combustion of solid rocket propellant. They impregnated the fuel under test with YAG:Dy, and used the ratio of an F-level band at 496 nm to a G-level band at 467 nm as the signal of interest. Because of thermalization, the intensity of the 467-nm band increased in comparison with the 496-nm band over the range from ambient to the highest temperature they were able to attain, 1,673 K. At that temperature, the blackbody emission introduces a significant background component into the signal, even within the narrow passband of the spectrometer that was employed. To mitigate this, they used a Q-switched Nd:YAG laser (frequency-tripled to 355 nm). The detectors in this arrangement included an intensified (1024-element) diode array that was gated on for a period of $10 \mu\text{s}$. They also used an intensified CCD detector. To simulate combustion in the laboratory, the phosphor was mixed with a low melting point (400 K) plastic and the resulting blend was heated with a focused CO_2 laser which ignited a flame that eroded the surface. A time-history of the disintegrating plastic surface was then obtained with the measurement system. Because of the short duration of the fluorescence, the power of the laser, and the gating of the detector, they were able to measure temporally resolved temperature profiles in the presence of the flame.

Krauss, Laufer and colleagues at the University of Virginia have utilized laser-induced phosphor fluorescence imaging for temperatures as high as 1100 C. Their efforts over the past decade have included a simultaneous temperature and strain sensing method, which they have pioneered (18, 19). For this they deposit closely spaced

thin stripes of phosphor material on the test surface. A camera views laser-induced fluorescence from the stripes. An image is acquired at ambient, unstressed conditions and subsequently at temperature and under stress. A digital moiré of the stripes is produced by comparing the before and after images. The direction and magnitude of the moiré patterns indicate strain. The ratio of the two colors of the fluorescence yields temperature.

C. Pressure-Sensitive Paint Applications

Background

Pressure-sensitive paints are coatings, which utilize luminescing compounds that are sensitive to the presence of oxygen. (20, 21) On the molecular level, a collision of an oxygen molecule prevents fluorescence, thus, the greater the oxygen concentration, the less the fluorescence. This is a newer application of fluorescence than planar LIF and thermography, but it is a field of rapidly growing importance. The prospect for imaging pressure profiles of aerodynamic surfaces in wind tunnels and inside turbine engines, as well as in situ flights has spurred this interest.

For the isothermal case, the luminescence intensity, I , and decay time, τ , of a pressure sensitive paint depend on oxygen pressure as:

$$\frac{\tau_0}{\tau} = \frac{I_0}{I} = 1 + K \cdot P_o = 1 + k_q \tau_o P_o$$

Where $K = k_q \cdot \tau_0$ and the subscript 0 refers to the respective values at zero oxygen pressure (vacuum).

Temperature plays a role in the oxygen quenching as the collision rate is of course temperature dependent. The precise temperature dependence may be further complicated as there may be additional thermal quenching mechanisms and the absorption coefficient can be somewhat affected by temperature. In practice, rather than performing the measurements at vacuum, a reference image is taken at atmospheric conditions where pressure and temperature are well established. The common terminology is “wind-on” and “wind-off”. The equations may then be rearranged to obtain:

$$\frac{I_{REF}}{I} = A(T) + B(T) \cdot \frac{P}{P_{REF}}$$

Pressure-sensitive paint installations typically utilize an imaging system with a CCD camera connected to a personal computer with some type of frame digitizing hardware. Illumination may be provided with any of a variety of mercury or rare-gas discharge lamps, pulsed or continuous. Laser beams may be used which are expanded to fully illuminate the object. Alternatively the lasers are scanned as described above in the planar LIF section.

Review of PSP

There are several reviews in this rapidly developing field (20-22). Some of the most important initial work using oxygen-quenched materials for aerodynamic pressure measurements was performed by Russian researchers in the early 1980's. (23). In the United States the method was pioneered by researchers at the University of Washington and collaborators (24, 25) In the early 1990's, the PSP's became a topic for numerous conference presentations where it was applied to a wide range of low speed, transonic, and supersonic aerodynamic applications. Measurement of rotating parts is important and is one requirement driving the search for short decay time luminophors. The other is the desire for fast temporal response of the sensor. Laboratory setups can be compact, simple and inexpensive. On the other hand, a 16 ft diameter wind tunnel at the Air Force's Arnold Engineering Development Center boasts of numerous cameras viewing the surface from a variety of angles (26). In this latter application, significant progress has been achieved in computational modeling for removing various light scattering effects that can be significant for PSP work. (27)

The collective experience from nonimaging applications of PSP's and TSP's shows that either decay time or phase measurement usually presents the best option for determining pressure (or temperature) due to immunity from various noise sources and inherently better sensitivity. Therefore, phase sensitive imaging and lifetime imaging are approaches that are being explored and could prove very useful (28, 29).

Research into improved PSP material is proceeding in a variety of directions. Various biluminophor schemes are being investigated for establishing temperature as well as pressure. Phosphors and laser dyes are receiving attention as TSP's. Not only is the fluorescing material important but the host matrix is as well. The permeability to oxygen of the host governs the response to pressure changes. Thus, there is a search for new host materials to enable faster

response. For aerodynamic applications, the method for coating surfaces is very important. This is especially important, especially for scaled studies of aerodynamic heating and other effects dependent on model surface properties. Work at NASA Langley in this area utilizes both phosphors and pressure sensitive paints. (30,31).

Future Advances

Every advance in spectroscopy increases the number of applications for planar laser induced fluorescence. One of the main technological drivers for this is laser technology. The varieties of lasers available to the user continues to proliferate. As a given type of laser becomes smaller and less expensive, its utility to PLIF applications is expanded, sometimes facilitating the movement of a technique out of the lab and into the field. New laser sources always enable new types of spectroscopies and new spectroscopic information that can be exploited by PLIF. Improvements in producing narrower bandwidths, shorter pulse lengths, higher repetition rates, better beam quality, and wider frequency range, as the case may be, will aid PLIF.

In contrast, phosphor thermometry and pressure-sensitive paint applications usually only require a laser for situations requiring a high intensity due to remote distances, the need to use fiberoptics to access difficult to access surfaces. Those situations usually do not involve imaging. Improvements to incoherent light sources will likely have a greater impact on PT and PSP. For example, blue LEDs are sufficiently bright for producing useful fluorescence and are available commercially in arrays for spectroscopic applications. The trend will be to increased output and shorter wavelengths. However, one area of laser technology that could have a significant impact is the development of inexpensive blue and ultraviolet diodes.

The field of PSP application is the newest of the technologies discussed here and it has been growing the fastest. Currently applications are limited to pressures a few atmospheres. Since PSPs used to date are organic materials, the temperatures at which they can operate and survive are limited to about 200 C. Development of inorganic salts and other materials are underway for increasing the temperature and pressure range accessible to the technique.

It will not be the case that one PSP material will ever serve all possible needs. There may eventually be hundreds of PSP materials which may be selected on the basis of 1) chemical compatibility in the intended environment, 2) the need to match excitation and emission spectral characteristics with available light sources, 3) decay time considerations, important for moving surfaces, 4) pressure and temperature range, 5) frequency response required, 6) the specifics of adhesion requirements in the intended application, and possibly other considerations. The PSP materials of today are, to our knowledge, all based on oxygen quenching. However, materials will be developed which are sensitive to other substances as well.

References

1. W. P. Partridge, Experimental Assessment and Enhancement of Planar Laser-Induced Fluorescence Measurements of Nitric Oxide in an Inverse Diffusion Flame, Doctoral Dissertation, Purdue University, 1996.
2. D. L. Hartley, Laser Raman Gas Diagnostics, M. Lapp and C. M. Penney eds., Plenum, New York, NY.
3. M. Alden and S. Svanberg, Proceedings of the Laser Institute of America, Vol 47 Laser Diagnostics and Photochemistry, 134-143, 1984.
4. R. B. Miles, E. Udd, and M. Zimmerman, Appl. Phys. Lett. 32, 317-319, 1978.
5. R. K. Hanson, J. M. Seitzman, and P. H. Paul, Appl. Phys. B, 50, 441-454, 1990.
6. P. H. Paul, J. A. Gray, J. L. Durant, and J. W. Thoman, AIAA J. 32,1670-1675, 1994.
7. P. Partridge and N. M. Laurendeau, to be published in Applied Physics B.
8. Instrumentation for Flows with Combustion, A. M. K. P. Taylor, ed. Academic Press, 1993.
9. W. Demtroder, Laser Spectroscopy, Basic Concepts and Instrumentation, Pringer-Verlag, New York, NY, 1988.
10. N. M. Laurendeau, Prog. Energy Combust. Sci. 14, 147-170, 1988.
11. A. C. Eckbreth, Laser Diagnostics for Combustion Temperature and Species, Abacus Press, Cambridge, CA
12. R. M. Measures, J. Appl. Phys. 39, 5232-5245, 1968.
13. Flow Visualization VII : Proceedings of the Seventh International Symposium on Flow Visualization by J. P. Crowder (Editor), 1995.
14. K. T. V. Grattan and Z. Y. Zhang, *Fiber Optic Fluorescence Thermometry* (Chapman & Hall, London, 1995).
15. S. W. Allison and G. T. Gillies, Rev. Sci. Instrum. 68(7), pp. 1-36, July 1997.
16. D. J. Bizzak and M. K. Chyu, Rev. Sci. Instrum. **65**, 102 (1994).
17. P. Goss, A. A. Smith, and M. E. Post, Rev. Sci. Instr. **60**(12), pp. 3702-3706, 1989.
18. Marino, R. P.; Westring, B. D.; Laufer, G.; Krauss, R. H.; and R. B. Whitehurst, AIAA J. Vol. 37, 1097-1101, 1999.
19. A. C. Edge, G. Laufer, and R. H. Krauss, Applied Optics, Vol. 39(4), pp. 546-553, Feb. 1, 2000.
20. T. Liu, B. Campbell, S. Burns, and J. Sullivan, Applied Mechanics Reviews, 50(4), 227-246, 1997.
21. V. Mosharov, V. Radchenko, and S. Fonov, Luminescent Pressure Sensors in Aerodynamic Experiments, published by the Central Aerohydrodynamic Institute and CW 22 Corporation, Moscow, Russia, 1997.
22. B. G. McLachlan, and J. H. Bell, Experimental Thermal and Fluid Science, 10(4), 470-485, 1995.
23. M. M. Ardasheva, L. B. Nevshy, G. E. Pervushin, J. Appl. Mech. & Tech. Phys. 26(4), 469-474, 1985.
24. M. Gouterman, Jour. Chem. Ed. 74(6) 1997.
25. J. Kavandi et al. AIAA Paper 90-1516, 1990.
26. M. E. Sellers and J. A. Brill, AIAA Paper 94-2481, 1994.
27. W. Ruyten, Rev. Sci. Instrum. 68(9), 1997.
28. C. W. Fisher, M. A. Linne, N. T. Middleton, G. Fiechtner, and J. Gord, AIAA Paper 99-0771.
29. P. Hartmann and W. Ziegler, Anal. Chem. 68, 4512-4514, 1996.
30. G. M. Buck, "Quantitative Surface Temperature Measurement using Two-Color Thermographic Phosphors and Video Equipment," U.S. Patent No. 4 885 633 (5 December 1989).
31. G. M. Buck, J. Spacecraft Rockets, 32(5), 1995.

Oak Ridge National Laboratory, managed by UT-Battelle, LLC, for the U.S. Dept. of Energy under contract DE-AC05-00OR22725.

List of Figures.

Figure 1. Representative PLIF configuration. (99-1476.jpg)

Figure 2. Simple lens imaging. (2000-1086.jpg)

Figure 3. Line focus with a cylindrical lens. (2000_1087.jpg)

Figure 4. $\text{Gd}_2\text{O}_2\text{S:Tb}$ spectrum. (99-1479.jpg)

Figure 5. Intensity ratio versus temperature. (99-1477.jpg)

Figure 6. A phosphor imaging system. (2000-1084.jpg)

Figure 7. False-color thermograph of heated turbine blade. (99-1480C.jpg)

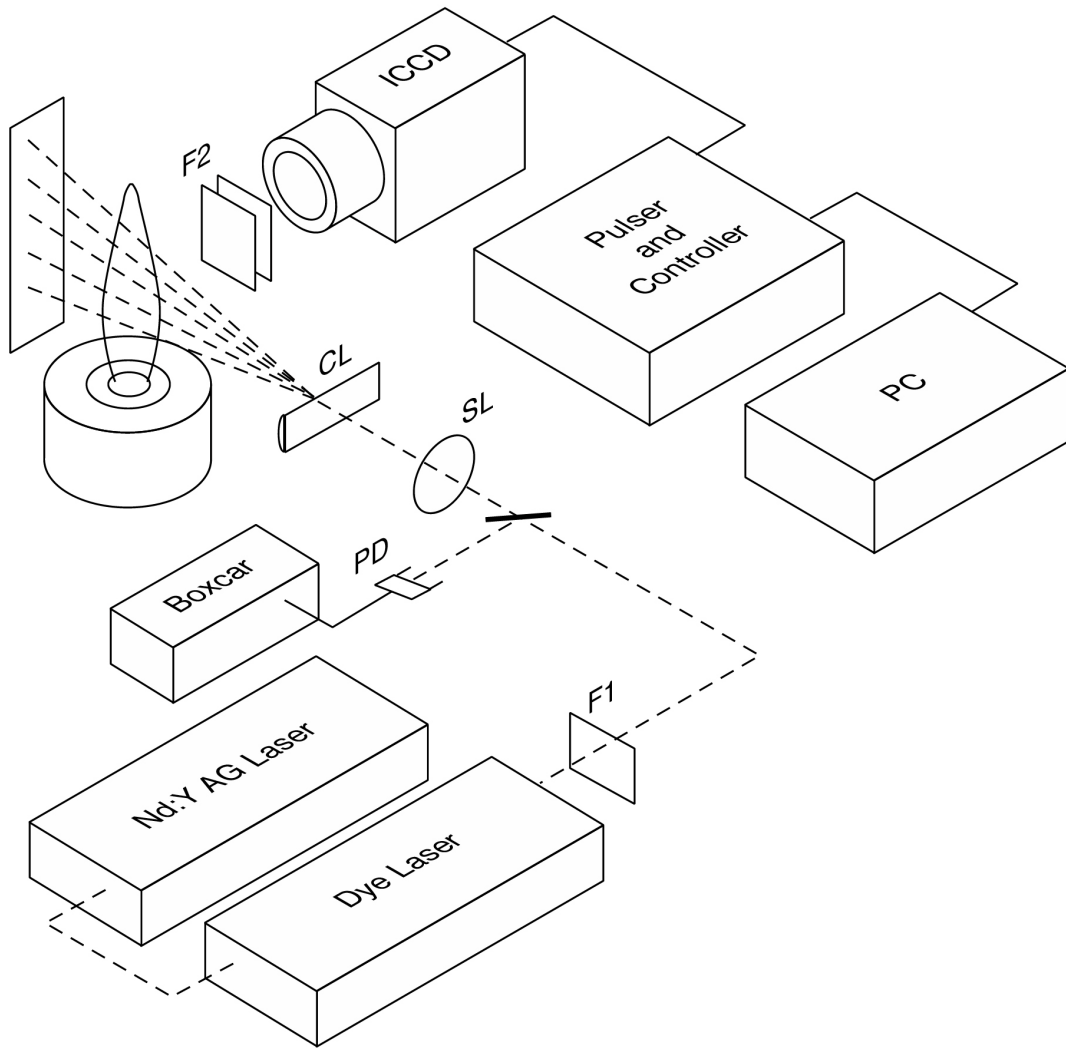


Figure 1. Representative PLIF configuration.

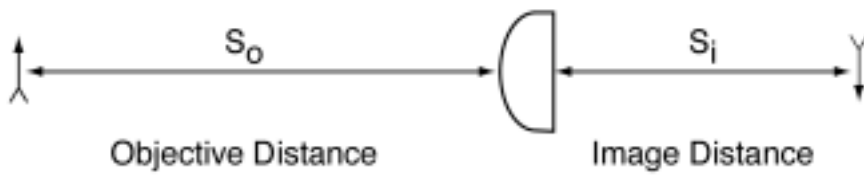


Figure 2. Simple lens imaging.

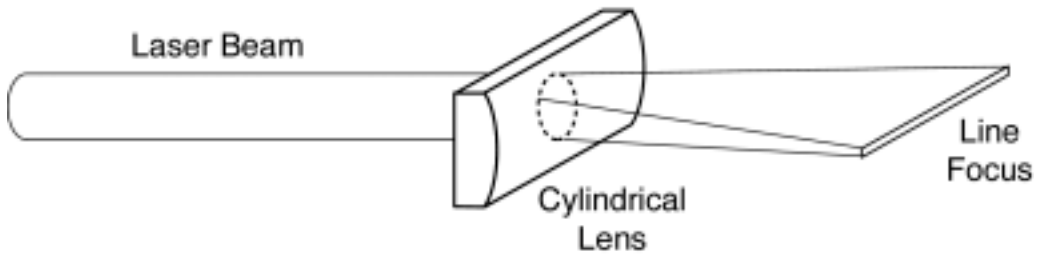


Figure 3. Line focus with a cylindrical lens.

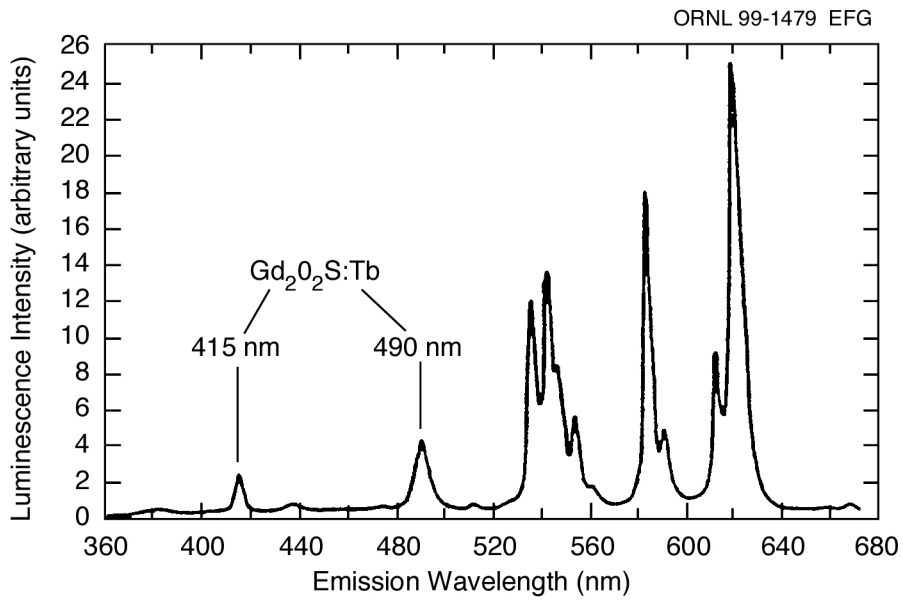


Figure 4. Gd₂O₂S:Tb spectrum.

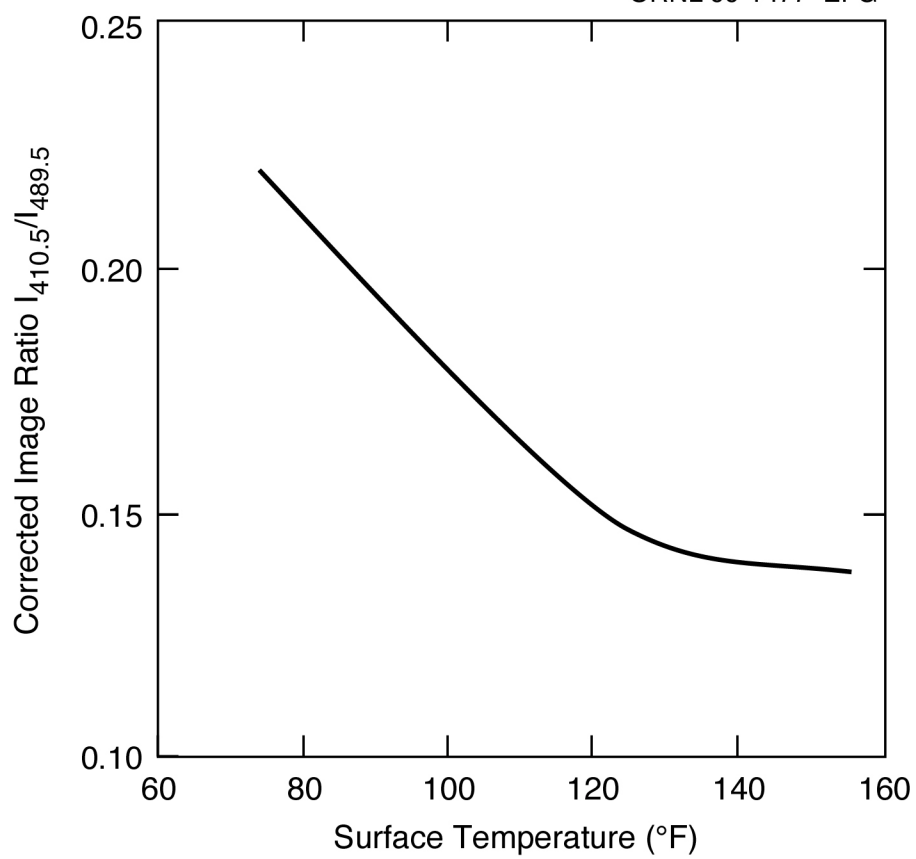


Figure 5. Intensity ratio versus temperature.

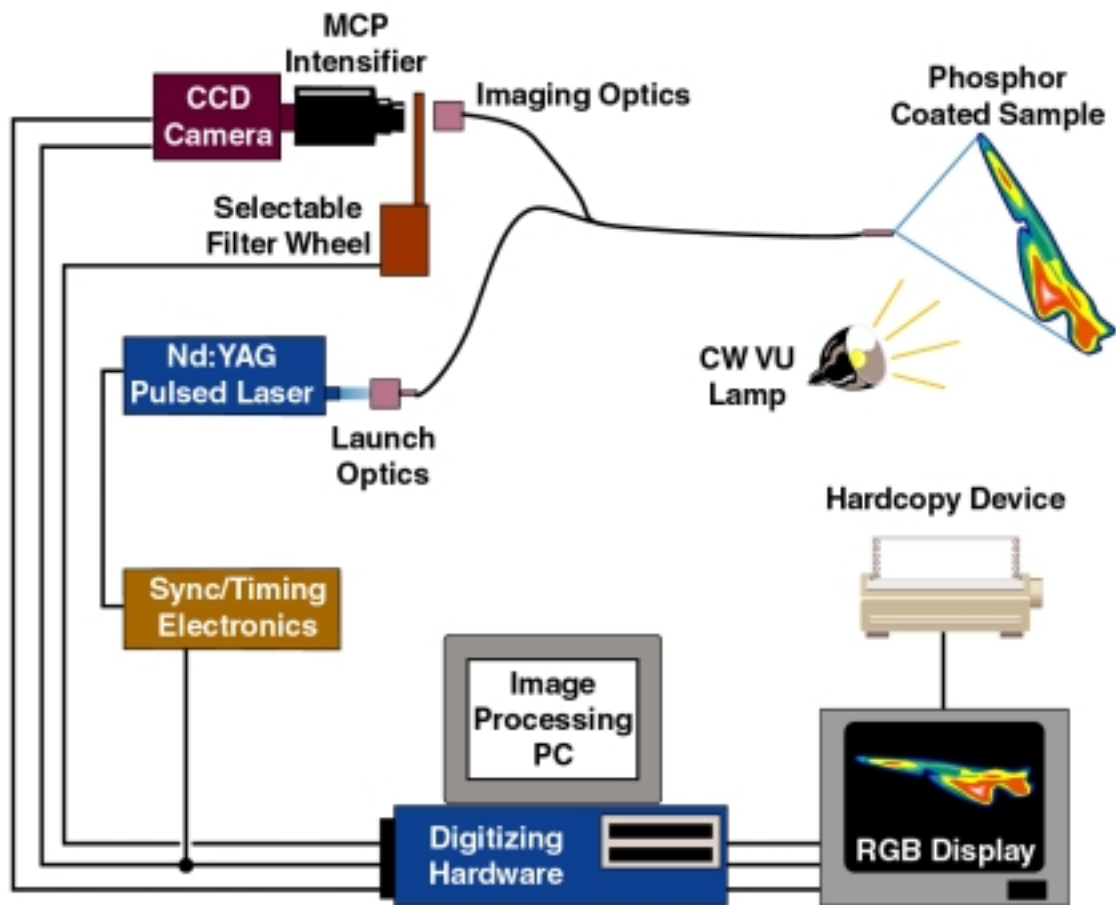
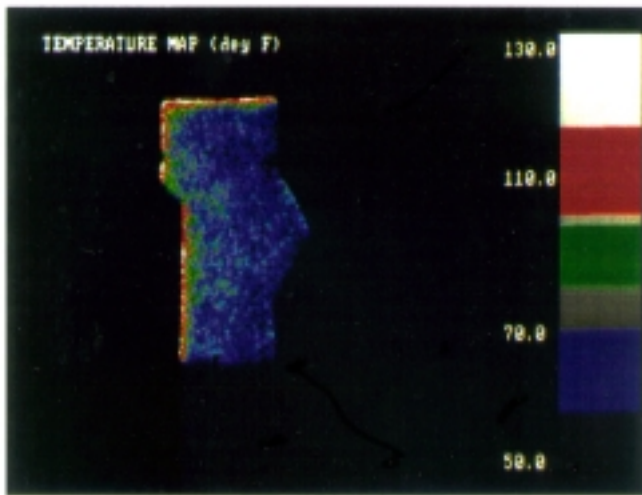
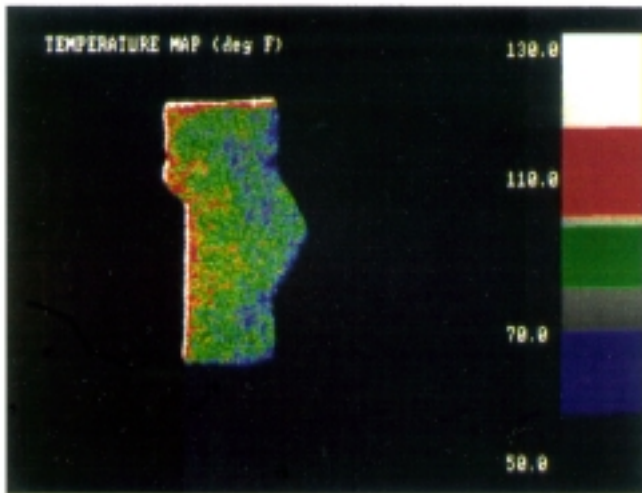


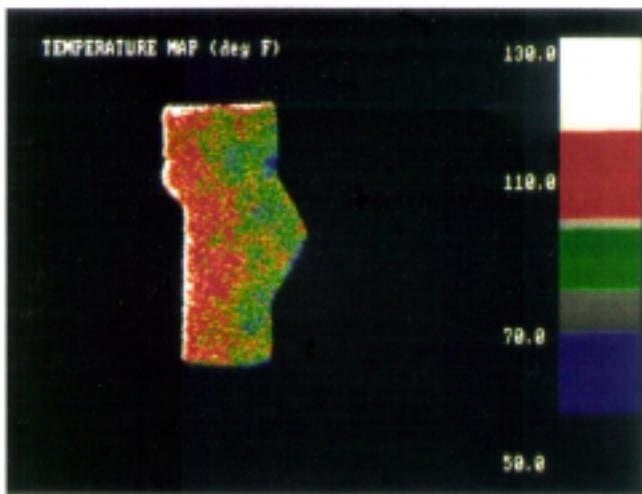
Figure 6. A phosphor imaging system.



(a)



(b)



(c)

Figure 7. False-color thermograph of heated turbine blade.